Ocean Engineering 80 (2014) 1–12

Contents lists available at ScienceDirect

Ocean Engineering

journal homepage: www.elsevier.com/locate/oceaneng

Prebreaking internal velocity field induced by a solitary wave propagating over a 1:10 slope

Chang Lin, Po-Hung Yeh*, Shih-Chung Hsieh, Ya-Ning Shih, Li-Fang Lo, Ching-Piao Tsai

Department of Civil Engineering, National Chung Hsing University, Taichung 402, Taiwan

ARTICLE INFO

Article history:
Received 29 July 2013
Accepted 28 January 2014
Available online 24 February 2014

Keywords:
Solitary wave
Wave shoaling
Runup
Rundown
PIV

ABSTRACT

The purpose of this study is to investigate the characteristics of the internal velocity field induced by a solitary wave propagating over a 1:10 slope. Flow visualization techniques and high time-resolved particle image velocimetry (PIV) were performed to resolve the velocity field. Different ratios of wave height to water depth as incident wave conditions were applied in the experiments. Test results show that the maximum runup velocity increases gradually along the slope before the solitary wave reaches its breaking point. Similarity of the velocity profile in the prebreaking area among different wave conditions can be obtained if adequate velocity and length scales are employed. Characteristics of the maximum negative velocity of the rundown flow were also studied. After carefully choosing its position reference, similarity of the maximum adverse velocity profile can be obtained as well.

1. Introduction

Tsunami and the resulting hazards have been a great concern in years, especially after the miserable disasters happened in Indonesia and Japan. When tsunami waves transverse the ocean from deep water to nearshore, wave height increases significantly and wave energy accumulates. After breaking around the shoreline, the subsequent wave runup can form a strong surge and bring a large amount of momentum and flood inland to cause nearshore structure damage and causalities. For example, the 2011 Tohoku Earthquake in Japan had triggered tsunami waves that reached heights of up to 40 m, and traveled up to 10 km inland (Mori et al., 2011). As reported by Japanese Government, the Tohoku Tsunami has caused about 130,000 buildings damaged or destroyed, and 25,000 people killed. Since most of the damage associated with tsunamis is related to the wave runup and rundown around the shoreline, understanding the velocity field variation during the whole process is important and critical for the assessment of any sort of mitigation effort.

Solitary wave theory has been widely applied to model tsunamis both in physical modeling and numerical simulations in related research communities since 1970s. Although its adequacy has been challenged by some new findings and arguments in recent studies (Madsen et al., 2008; Chan and Liu, 2012), investigations of a shoaling solitary wave through laboratory experiments still can provide some good insights, especially on the inland inundation and coastal region erosion caused by wave runup and rundown. Numerous laboratory experiments have been conducted to investigate the topic of solitary wave shoaling over a slope (Ippen and Kulin, 1954; Kishi and Saeki, 1966; Synolakis and Skjelbreia, 1993; Grilli et al., 1994, 2004; Lin et al., 1999; Jensen et al., 2005; Hsiao et al., 2008; Chang et al., 2009). Synolakis and Skjelbreia (1993) identified four different regions for the variation of maximum amplitude of a solitary wave, from shoaling, through breaking, to runup. These regions are gradual shoaling, rapid shoaling, rapid decay, and gradual decay, consecutively. Lin et al. (1999) presented the combined experimental and numerical studies to investigate solitary wave runup and rundown on steep and mild beaches. Velocity distribution and free surface profiles were discussed in their study. However, for the mild slope situation, only the free surface displacements were measured. Other properties, such as mean velocity field were obtained through numerical simulations. Hsiao et al. (2008) demonstrated laboratory experiments of solitary waves propagating on a 1:60 plane beach conducted in a super tank (300 m × 5 m × 5.2 m). Although breaking criterion, amplitude evolution and run-up height were all discussed in this study, shoreline motion and underwater particle velocity were only briefly discussed.

The objective of this paper is to investigate the internal velocity field of a shoaling solitary wave, through a series of delicate laboratory tests. These tests were conducted with the applications of flow visualization techniques and high time-resolved particle image velocimetry (PIV). Exclusive focus of this study was on the velocity field in the region before the wave breaking point.

* Corresponding author.
E-mail address: kuroshio@gmail.com (P.-H. Yeh).

http://dx.doi.org/10.1016/j.oceaneng.2014.01.017
0029-8018

Temporal variations starting from wave shoaling, through wave breaking, wave runup and finally to wave rundown were discussed. Similarity profiles of the maximum runup and rundown velocities were analyzed. This study also aims to expand the data bank of velocity measurements under a shoaling solitary wave. It would be useful in other applications, such as numerical simulations and tsunami mitigation assessments.

2. Experimental setup and measurement systems

2.1. Experimental setup

The experiments were conducted in a wave flume at the Department of Civil Engineering, National Chung Hsing University, Taiwan. The flume was of 14 m long, 0.25 m wide and 0.5 m deep, with glass bottom and sidewalls. A piston-type wave generator controlled by computer-programmed analog input signals was installed at one end of the flume. Simulating solitary waves were then generated towards the opposite side of the flume, against a model slope which was 9 m away from the wave generator. The model slope was made of acrylic with an adjustable frame to change its slope; however, a 1:10 slope was fixed throughout the entire study. As shown in Fig. 1(a), a Cartesian coordinate system was employed with the origin $(x, y)=(0, 0)$ at the toe of the model; positive x and y directions were defined as the horizontal and vertical directions to the flume, respectively. The water particle velocities in these two directions were denoted as u and v, and the resultant magnitude of velocity $V=\sqrt{u^2+v^2}$. h_0 and H_0 were the still water depth and non-shoaling solitary wave height in the constant-depth part of the flume, while $\eta(t, x)$ and $h(x)$ were the local free surface elevation and water depth on the slope.

Seven cases of different solitary wave height to water depth ratios H_0/h_0, ranging from about 0.1 to 0.4, were tested to give the largest possible coverage of this ratio according to the capability of the wave generator and other facility constraints. Table 1 lists the incident wave conditions. Note that the wave celerity c_0 in the table were calculated from wave gauge measurements (will be discussed later). In addition, t was time and a non-dimensional time $T[=t(g/h_0)^{1/2}]$ was defined as $T=0$ (also $t=0$) when the solitary wave crest was right at $x=0$.

2.2. PIV system and FOVs

The PIV system was used to measure the two-dimensional velocity field induced by the solitary waves when propagating over the slope. It consists of a Argon-Ion laser (Innova-300 of Coherent Inc.) as light source, and a high-speed camera (Phantom V5.1 of Vision Research) to capture images. The laser system has 7 W maximum energy output in the wavelength range of 457.9–514.5 nm. A set of optical lens was used to diverge the laser beam into a light sheet of approximately 1 mm thickness, and redirect it to enter the flume vertically through the glass bottom along the flume centerline. The intensity of the light sheet is not disturbed by the fluctuating free surface if entering the water column from the flume bottom.

The high-speed camera used in the experiments was capable of capturing sediment-laden images with a highest 1200 Hz framing rate. Each image was set having 1024 × 1024 pixel resolution with 10-bit dynamic range. A Nikon 105 mm f/2.8D AF Micro-Nikkor lens was mounted on the camera. In addition to PIV measurements, the camera was also used to conduct qualitative flow visualization. Seeding particles were introduced into water and illuminated by the laser light sheet. Particle trajectories were then captured using the camera with a controlled exposure time between 10 μs and 47,000 μs. Titanium Dioxide (TiO_2) powder (specific gravity 4.28, particle diameter 1 μm) was chosen as the tracing particles. Its refractive index and falling velocity were 2.60 and 2.32 μm/s, respectively.

In order to have higher spatial resolution, six fields of view (FOV) were employed on the slope for the image-based visualization and PIV measurements. Each FOV was of 10 cm × 10 cm area, and the center of the first FOV was placed at $x=34$ cm. Other FOVs were shifted subsequently 8 cm in the $+x$ direction. A 2-cm overlapping between two FOVs improved resolution and accuracy in the areas close to the FOV edges. The whole field of view was of 48 cm range covering from $x=30$ cm to $x=78$ cm on the slope in the investigations. The schematic diagram of the six FOVs is shown in Fig. 1(b).

Table 1
Experimental conditions.

Case name	Wave height H_0 (cm)	Water depth h_0 (cm)	H_0/h_0	Wave celerity c_0 (cm/s)
A	1.3	10	0.133	104.9
B	1.2	7	0.176	90.1
C	1.5	7	0.210	90.9
D	2.1	8	0.262	98.0
E	1.9	7	0.275	93.5
F	2.9	8	0.359	102.0
G	2.7	7	0.384	99.0

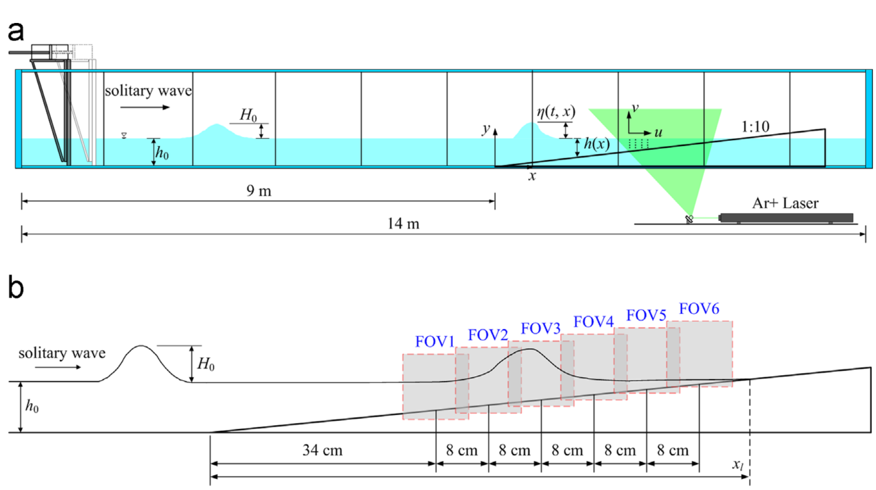

Fig. 1. (a) Experimental setup and (b) sketch of the six FOVs on the slope.